MOLECULAR AND CELLULAR BIOLOGY, June 1999, p. 4379–4389 Vol. 19, No. 6
0270-7306/99/$04.00+0

Ajuba, a Novel LIM Protein, Interacts with Grb2, Augments Mitogen-Activated Protein Kinase Activity in Fibroblasts, and Promotes Meiotic Maturation of *Xenopus* Oocytes in a Grb2- and Ras-Dependent Manner

RAKESH K. GOYAL,[1]† PHOEBE LIN,[2] JOSNA KANUNGO,[2] AIMEE S. PAYNE,[3] ANTHONY J. MUSLIN,[2,3] AND GREGORY D. LONGMORE[2,3]*

Departments of Pediatrics,[1] Medicine,[2] and Cell Biology,[3] Washington University School of Medicine, St. Louis, Missouri 63110

Received 25 August 1998/Returned for modification 22 October 1998/Accepted 8 February 1999

LIM domain-containing proteins contribute to cell fate determination, the regulation of cell proliferation and differentiation, and remodeling of the cell cytoskeleton. These proteins can be found in the cell nucleus, cytoplasm, or both. Whether and how cytoplasmic LIM proteins contribute to the cellular response to extracellular stimuli is an area of active investigation. We have identified and characterized a new LIM protein, Ajuba. Although predominantly a cytosolic protein, in contrast to other like proteins, it did not localize to sites of cellular adhesion to extracellular matrix or interact with the actin cytoskeleton. Removal of the pre-LIM domain of Ajuba, including a putative nuclear export signal, led to an accumulation of the LIM domains in the cell nucleus. The pre-LIM domain contains two putative proline-rich SH3 recognition motifs. Ajuba specifically associated with Grb2 in vitro and in vivo. The interaction between these proteins was mediated by either SH3 domain of Grb2 and the N-terminal proline-rich pre-LIM domain of Ajuba. In fibroblasts expressing Ajuba mitogen-activated protein kinase activity persisted despite serum starvation and upon serum stimulation generated levels fivefold higher than that seen in control cells. Finally, when Ajuba was expressed in fully developed *Xenopus* oocytes, it promoted meiotic maturation in a Grb2- and Ras-dependent manner.

The LIM domain defines a unique double zinc finger structure found in a class of proteins involved in cell identity, differentiation, and growth control (10, 33). The LIM motif, $CX_2CX_{16-23}HX_2CX_2CX_2C\text{-}X_{16-21}CX_2C$(D,H), was initially identified in three developmentally important transcription factors, *Caenorhabditis elegans* Lin-11, rat Isl-1, and *C. elegans* mec-3, from which the acronym LIM is derived (16, 20, 41). LIM domains are highly conserved among proteins present in organisms representing an extensive range of evolution. They are thought to function as versatile protein modules, capable of acting within diverse cellular contexts and in multiple subcellular compartments. Many have been shown to participate in direct protein-protein interactions, and they may also have the capacity to bind DNA directly (5, 17, 34). Structural analysis of LIM domains suggest that most adopt a similar zinc-bound finger; however, no protein has been identified as a common target for LIM domains (28).

LIM domain-containing proteins have been classified according to the sequence homologies among the LIM domains and the overall structure of the protein (10). Group 1 proteins contain LIM domains linked to a homeodomain and a potential transcription activation domain. Examples include the three founder LIM proteins Lin-11 (16), Isl-1 (20), and mec-3 (41) and represent a growing group of nuclear transcription factors involved in cell fate determination and differentiation. Group 2 proteins are LIM-only (LMO) proteins consisting of one to five LIM domains without additional structural or functional motifs. These proteins can be nuclear (e.g., the erythrocyte protein rhombotin 2 or LMO2) (40), cytosolic (e.g., muscle cell cysteine-rich protein) (5), or both (e.g., myogenic LIM protein) (3). Group 3 proteins contain three to four tandem LIM domains at the C terminus in association with distinct N-terminal domains. Members of this group include zyxin (9), Enigma (45), paxillin (38), lipoma partner protein (29), Trip6 (23), and the protozoal proteins AvL3-1 and OvL3-1 (27). Proteins not conforming to definitions of groups 1 to 3 constitute a fourth or other group. Some contain functional serine/threonine kinase domains and have been termed LIM kinases (25).

All group three LIM proteins are cytosolic. The LIM domains of these proteins have been shown to interact with cell surface proteins (e.g., Enigma) (12, 45), cytoskeletal proteins at sites of cell adhesion (e.g., zyxin and paxillin) (4, 37), or other LIM proteins (e.g., zyxin) (31). In addition to their LIM domains, group 3 proteins contain extensive N-terminal non-LIM, or pre-LIM, domains that are quite divergent in sequence. All, however, are rich in proline residues, with some proline-rich stretches conforming to consensus SH3 recognition sites (1, 15). Indeed, some have been shown to interact with the SH3 domains of various cytosolic proteins in vitro (18, 43). However, the functional significance of these interactions in vivo has not been demonstrated. In addition, the pre-LIM domain of zyxin also mediates an interaction with α-actinin and members of the VASP protein family that are important for the assembly and maintenance of the actin cytoskeleton (30).

In this report we describe the isolation and characterization of a new group 3 LIM protein, Ajuba. Ajuba contains three tandemly arranged LIM domains in the C-terminal region. The

* Corresponding author. Mailing address: Division of Hematology, Washington University School of Medicine, Campus Box 8125, 660 South Euclid Ave., St. Louis, MO 63110. Phone: (314) 362-8834. Fax: (314) 362-8826. E-mail: longmorg@medicine.wustl.edu.

† Present address: Department of Pediatrics, University of Pittsburgh, Pittsburgh, PA 15213-2583.

amino-terminal pre-LIM domain is abundant in glycine and proline residues. There are two potential SH3 recognition motifs within the pre-LIM domain. We show that Ajuba associates with Grb2 in vitro and in vivo. This interaction was mediated by the pre-LIM domain of Ajuba and the SH3 domains of Grb2. Expression of Ajuba in fibroblasts resulted in enhanced mitogen-activated protein (MAP) kinase activity. The functional significance of this interaction was evident when murine Ajuba was expressed in fully developed *Xenopus* oocytes. Meiotic maturation, in response to progesterone and insulin, was promoted in a Grb2- and Ras-dependent manner.

MATERIALS AND METHODS

Cell lines and antiserum. Embryonic stem (ES) cells were maintained and differentiated into embryoid bodies by the suspension culture method (11). F9 teratocarcinoma and NIH 3T3 fibroblast cell lines were maintained in culture as described elsewhere (19). Rabbit polyclonal antiserum was generated against the 13-amino-acid C-terminal peptide (QRLSARQPSTNYI) of Ajuba by QCB Biochemicals (Hopkinton, Mass.). Immune serum was affinity purified by passing serum over an immunogen peptide-sulfo-link column (Pierce). Antiserum was characterized through immunoblotting of ES cell extracts or immunoprecipitation of products from in vitro-translated Ajuba cDNA as described below. Rabbit polyclonal anti-Myc antiserum was generated by A. Shaw (Washington University). Grb2, ERK, and paxillin antisera were obtained from Santa Cruz Biotechnology (Santa Cruz, Calif.). Antiserum specific for activated MAP kinase was obtained from New England Biolabs (Beverly, Mass.). Rabbit polyclonal anti-glutathionine *S*-transferase (GST) antiserum was produced by J. Cooper (Washington University). GST-Grb2 and GST-Grb2 SH3-N,C have been described elsewhere (36). GST-Grap, GST-Grap SH3-N, and GST-Grap SH3-C are described in reference 14.

cDNA cloning and sequencing. A yeast two-hybrid strategy was used to screen an embryonic day 9.5 (E9.5) total mouse embryo small-fragment cDNA library (39) by using the 42-amino-acid carboxy-terminal end of the mouse erythropoietin receptor (EPO-R) as bait. From 500,000 clones screened, 22 primary positives were identified. Of these, four were found to specifically interact with the EPO-R peptide in yeast. Two were overlapping clones of a single cDNA. One of these, a 554-bp partial clone, was sequenced and used to isolate the full-length clone from an E6.5 total mouse embryo cDNA library, kindly provided by John D. Gearhart, Baltimore, Md. (42). Using the Exassist in vivo excision protocol (Stratagene), pBluescript (pBS) phagemids were prepared from the positive clones identified. Sequence analysis of both strands of isolated clones was performed by the dideoxynucleotide method using Taquence (U.S. Biochemicals). Sequence similarity searches were performed on the BLAST server, using the nonredundant database at the National Center for Biotechnology Information, National Institutes of Health.

Northern blot analysis. RNA was isolated by using RNA STAT-60 (Tel-Test). Twelve micrograms of total RNA was subjected to formaldehyde-agarose gel electrophoresis, transferred to a Zetabind membrane, and hybridized with ^{32}P-labeled probes according to the manufacturer's guidelines (CUNO Inc.). Fragments of the Ajuba cDNA used as probes on Northern blots included a 439-bp piece from the 5′ untranslated region region (nucleotides 64 to 503), a 612-bp piece at the 5′ end of the coding region (nucleotides 504 to 1116), and a 554-bp piece from the 3′ LIM region (nucleotides 1119 to 1673). Equivalent sample loading was assessed by stripping blots and reprobing with actin or comparative assessment of ethidium bromide-stained 28S and 18S rRNAs.

Immunoprecipitation. For in vitro transcription and translation, Ajuba cDNA was subcloned into pBS (Stratagene) in an orientation whereby sense-strand transcription was driven by T7; in vitro transcription reactions were performed according to manufacturer's recommendations, using the T7 promoter and a wheat germ agglutinin transcription/translation system (TNT; Promega). During the translation reaction, proteins were metabolically labeled with [^{35}S]methionine-[^{35}S]cysteine. Products were separated by sodium dodecyl sulfate-polyacrylamide gel electrophoresis (SDS-PAGE) under reducing conditions, or diluted in radioimmunoprecipitation assay (RIPA) buffer, and immunoprecipitated with specific Ajuba antiserum, or preimmune serum, and protein A-agarose prior to separation by SDS-PAGE.

Generation of NIH 3T3 cells containing Ajuba proteins. To prepare Myc-tagged eukaryotic expression plasmids, PCR fragments corresponding to full-length Ajuba, pre-LIM Ajuba (amino acids 2 to 340), and the three LIM domains of Ajuba (amino acids 340 to 547) were subcloned, in frame, into plasmid pCS2, which contains an N-terminal penta-Myc tag, provided by R. Kopan (Washington University, St. Louis, Mo.). All constructs generated through PCR-based strategies were verified by dideoxynucleotide sequencing. To generate NIH 3T3 cells stably expressing the above Ajuba constructs, cells were transfected by using Lipofectamine (Gibco BRL) and selected in complete medium containing 800 μg of G418 (Gibco BRL) per ml. Clones were picked and expanded. Expression of the appropriate protein was confirmed through immunoblotting of cell extracts with rabbit polyclonal anti-Myc antiserum and, when applicable, with rabbit polyclonal anti-Ajuba antiserum.

Immunoblot analysis. All cell lines and tissues studied were washed in phosphate-buffered saline (PBS) and then lysed in lysis buffer (1% Triton X-100 or 1% Nonidet 40 [NP-40], 20 mM Tris-Cl [pH 7.4], 140 mM NaCl [Tris-buffered saline {TBS}], 5 mM EDTA) or RIPA buffer (1% NP-40, 0.5% sodium deoxycholate, and 0.1% SDS in phosphate-buffered saline [PBS; pH 7.4]) containing 1 mM sodium vanadate, 2 mM phenylmethylsulfonyl fluoride and 10 trypsin inhibitory units of aprotinin per ml for 15 min on ice. Lysates were clarified by centrifugation at 10,000 × *g* for 20 min, and the detergent-soluble supernatant was saved for further analysis. Detergent-soluble proteins were separated by SDS-PAGE under reducing conditions and transferred to nitrocellulose (Schleicher & Schuell). Membranes were incubated in TBS/T blocking solution (TBS [pH 7.4] containing 5% [wt/vol] milk and 0.1% [vol/vol] Tween 20 or TBS/T [pH 7.4] containing 3.0% [wt/vol] bovine serum albumin [BSA]), followed by incubation with primary antibodies. After washing in TBS/T, membranes were incubated with horseradish peroxidase-coupled donkey anti-rabbit or anti-mouse immunoglobulin G (IgG) (Amersham). Membranes were washed, and immunoreactive bands were visualized with enhanced chemiluminescence reagents (Amersham). Autoradiographs were scanned into Adobe Photoshop for production of figures.

Immunofluorescence. Regularly passaged NIH 3T3 cells were split, plated onto chamber slides (LabTek), and grown overnight in complete medium. The slides were then washed with PBS and fixed in 4% paraformaldehyde for 30 min at room temperature. Slides were blocked in 10% (vol/vol) goat or donkey serum, 0.5% (wt/vol) BSA, and 0.05% saponin in PBS for 30 min at room temperature. Cells were then incubated with primary antiserum in PBS–0.5% BSA–0.05% saponin for 1 h. Next cells were washed five times with PBS, and then fluorescein isothiocyanate-conjugated anti-rabbit or anti-mouse IgG (Cappel) or Cy3-conjugated antimouse IgG (Jackson Laboratories) was added. Slides were again washed five times in PBS, dried, mounted in antifade (Bio-Rad), and examined with a fluorescence microscope (Nikon). In some experiments, F-actin was visualized by adding rhodamine-phalloidin (Molecular Probes).

Preparation of fusion proteins and in vitro binding studies. To prepare GST fusion proteins, PCR fragments encoding the full-length Ajuba and EPO-R cDNAs, the three LIM domains of Ajuba, and the pre-LIM region of Ajuba were subcloned into the *Eco*RI site of pGEX2T 128/129 (Pharmacia). To ensure in-frame translation of the fusion proteins, all plasmid constructs were sequenced. *Escherichia coli* BL21 cells were transformed with these plasmids, selected, and induced to express the fusion proteins by incubation with 0.1 mM isopropyl-β-D-thiogalactopyranoside at 30°C overnight. Fusion proteins were purified from *E. coli* BL21 extracts with glutathione-agarose. Production of proteins of the appropriate size was confirmed by Coomassie staining of the gel after SDS-PAGE and immunoblotting of separated products with rabbit polyclonal anti-GST antiserum. GST-Grb2, GST-Nck, GST-Lck, and GST-Vav constructs were provided by A. Chan (Washington University) and B. Mayer (Harvard Medical School) (36). GST-Grap constructs were provided by Gen-Sheng Feng (Indiana University) (14).

For binding studies, cell extracts were prepared from cells growing exponentially in serum. Cells were harvested and lysed in 1% NP-40–20 mM Tris-Cl (pH 7.4)–140 mM NaCl containing 1 mM sodium vanadate, 2 mM phenylmethylsulfonyl fluoride, and 10 TIU of aprotinin per ml. Following clarification of extracts, lysates were precleared by adding purified GST and glutathione-agarose. Specific GST fusion proteins (1 to 5 μg) were added to clarified, precleared, detergent-soluble extracts from 1×10^7 to 2×10^7 cells and incubated for 2 h at 4°C. Glutathione-agarose was added, and incubations continued for another hour. Pellets were washed four times in lysis buffer, and bound products were resolved by SDS-PAGE, transferred to nitrocellulose membranes, and immunoblotted. Subsequently, blots were stripped and reprobed with anti-GST antiserum to ensure that equivalent amounts of fusion proteins were added per sample.

MAP kinase assays. NIH 3T3 clones expressing Mvc-Ajuba, Myc–pre-LIM Ajuba, LIM Ajuba, and empty vectors (3T3.Neo) were cultured in Dulbecco modified Eagle medium–50 mM HEPES (pH 7.4) for various periods of time. They were then either trypsinized, washed in PBS, and sonicated in 1× SDS sample buffer or stimulated with serum for 10 min and then trypsinized, washed, and sonicated in 1× SDS sample buffer. The protein concentration of each sample was determined by the Bio-Rad assay (Pierce). Equal amounts of protein was loaded in each lane, resolved by SDS-PAGE under reducing conditions, transferred to nitrocellulose, and immunoblotted with antiserum against activated MAP kinase (New England Biolabs). Subsequently blots were stripped and reprobed with anti-ERK1-ERK2 antiserum. Alternatively, cells were lysed in lysis buffer and the soluble fraction was immunoprecipitated with antiserum against ERK and protein A-agarose. Pellets were washed, and in vitro kinase reactions were performed in the presence of [γ-^{32}P]ATP and myelin basic protein (MBP) as the substrate. Products were resolved by SDS-PAGE under reducing conditions, the gel was dried, and autoradiography was performed.

Microinjection of *Xenopus* oocytes. To prepare mRNA for *Xenopus* oocyte expression, all constructs were subcloned into plasmid pCS2. Each plasmid was linearized; mRNA was produced by using SP6 RNA polymerase and capped with 5 mM diguanosine triphosphate according to Promega Riboprobe kit instructions. Following the reaction, template DNA was removed by treating the reaction products with DNase I (Promega) and extracted with phenol-chloroform,

FIG. 1. Nucleotide and derived amino acid sequences of murine Ajuba cDNA. Amino acids are numbered on the left, and nucleotides are numbered on the right. The three LIM domains are underlined. Potential SH3 recognition motifs are in bold type. A putative NES is underlined with a broken line.

and RNA was precipitated in ethanol. Samples were resuspended at a concentration of 1 μg/μl. RNA production was verified by agarose gel electrophoresis. Control mRNA was synthesized from a pCS2 plasmid lacking any cDNA insert.

Ovaries were surgically removed from mature *Xenopus* frogs, which had been anesthetized by hypothermia, and placed into medium containing 88 mM NaCl, 1 mM KCl, 2.4 mM $NaHCO_3$, 0.82 mM $MgSO_4$, 10 mM HEPES (pH 7.4), 0.33 mM $Ca(NO_3)2 \cdot 4H_2O$, 0.41 mM $CaCl_2 \cdot 2H_2O$, 1 g of BSA per liter, 1 g of Ficoll 400 per liter, and 10 μg of penicillin-streptomycin per ml. Oocytes were extracted from the ovarian follicles by incubation in 2 mg of collagenase (Sigma type I) per ml for 2 h. Fully grown stage VI oocytes were isolated and allowed to recover in medium at 19°C overnight. Oocytes were then injected with 50 nl of mRNA, allowed to recover (dead oocytes were removed), and incubated in 1 to 3 μM progesterone or insulin. At various times following the addition of progesterone or insulin, meiotic maturation was scored by observing germinal vesicle breakdown (GVBD). At various time points, individual oocytes were collected, lysed in 1× Laemmli sample buffer containing 2-mercaptoethanol, and analyzed for MAP kinase activity (see above) and for expression of Ajuba by immunoblotting.

Nucleotide sequence accession number. The GenBank accession no. for Ajuba is U79776.

RESULTS

Isolation and characterization of murine Ajuba cDNA. To identify candidate proteins interacting with a cytoplasmic C-terminal domain of the murine EPO-R, we used a yeast two-hybrid screen. From an E9.5 total mouse partial cDNA library (39), we identified four clones that specifically interacted with the EPO-R-derived protein in yeast. Two of these clones were overlapping partial cDNA clones that upon DNA sequencing were found to contain an open reading frame encoding for two LIM domains. To isolate the full-length cDNA encoding for Ajuba, a 554-bp partial cDNA piece was used to screen an E6.5 total mouse embryo phage cDNA library (42). The 2,984-nucleotide sequence of clone 3B is shown in Fig. 1.

The ATG at position 267 was presumed to be the start codon since it is flanked by the nucleotides that conform to the canonical eukaryotic translation initiation consensus sequence (22a), and stop codons are present in all three reading frames upstream of this site. In addition, upstream of this site is a GC (75%)-rich region of 266 nucleotides. The start site was followed by a single open reading frame of 1,638 nucleotides and a 3′ untranslated region of 1,074 nucleotides. The cDNA is predicted to encode a 547-amino-acid protein of approximately 58 kDa, which we have designated Ajuba ("curiosity" in Urdu, an Indian dialect). Examination of its deduced amino acid sequence revealed a number of salient features. First, the C-terminal third was rich in cysteine and histidine residues which were organized into three tandemly arrayed copies of LIM domains with highest homology to group 3 LIM proteins (44% identity and 65% similarity score with chicken zyxin) (9, 10). Second, the N-terminal two-thirds was rich in glycine and proline (16 and 11%, respectively). The abundance of glycine residues in the N terminus was unique and distinguishes Ajuba from other group 3 members, such as zyxin, Enigma, and

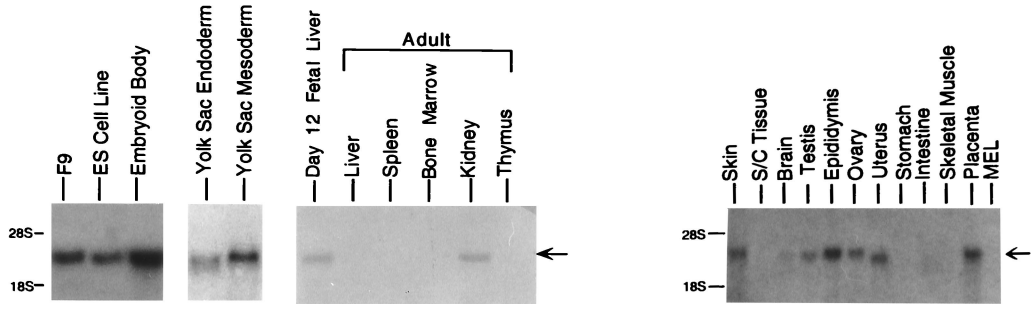

FIG. 2. Northern blot analysis for Ajuba mRNA expression in cell lines and tissues. Total RNA (12 μg) from each tissue was subjected to formaldehyde-agarose gel electrophoresis, transferred to a Zetabind membrane, and hybridized with a ^{32}P-labeled Ajuba partial cDNA probe corresponding to the pre-LIM domain. The arrows identify the 3-kb Ajuba mRNA.

paxillin. The abundance of proline residues is typical of group 3 LIM proteins; however, most have a higher percentage (15 to 25%). In addition, there were two stretches of proline-rich SH3 recognition motifs (1, 15). Third, there was a nuclear export signal (NES) motif, very much like the functional NES present in zyxin both in its location within the deduced sequence and in its sequence homology (7, 26). Finally, there were no stretches of hydrophobic amino acids, typically present in transmembrane proteins or indicative of signal sequences.

Tissue expression of Ajuba. Northern blot analysis for Ajuba gene expression was performed on embryonic and adult tissues and cell lines (Fig. 2). A single 3-kb transcript was present in totipotent ES cells, embryonic yolk sac endoderm and mesoderm cell lines, placenta, undifferentiated F9 teratocarcinoma cells, and E12.5 fetal liver. Induction of ES cell differentiation into embryoid bodies resulted in a threefold increase of Ajuba transcript. RNA in situ hybridization studies of developing mouse embryos (data not shown) revealed that in early postimplantation embryos (E7.5 to 8.5) Ajuba was present in all embryonic germ layers, in the extraembryonic yolk sac blood islands, and in the fetal components of the developing placenta. As development progressed, expression was dramatically restricted such that in maturing embryos (post-E12.5), Ajuba expression was limited to the skin, nervous system, and genitourinary tract. Among adult tissues, Ajuba was present in the skin, brain, and genitourinary organs (e.g., testis, epididymis, ovary, uterus, and kidney). No transcript was detected in adult subcutaneous tissue, bone marrow cells, liver, spleen, thymus, stomach, intestine, or skeletal muscle.

Ajuba is a 55-kDa protein. Rabbit polyclonal antiserum was generated against a carboxy-terminal peptide of Ajuba. In vitro-translated full-length Ajuba clone 3B produced a protein product of approximately 55 kDa (Fig. 3, lane 1). From the products of this in vitro translation reaction, anti-Ajuba immune serum precipitated a 55-kDa protein (lane 3), whereas preimmune serum did not react with any products (lane 2). Immune serum also specifically detected a 55-kDa protein in detergent-soluble cell extracts from F9 (data not shown) and ES (see Fig. 5A) cells. Thus, the immune serum specifically recognized a 55-kDa protein in cells expressing Ajuba mRNA.

When the full-length EPO-R and Ajuba proteins were coexpressed in cell lines, we did not detect an interaction between the two proteins (data not shown). In addition, GST fusion proteins of each protein did not interact with the reciprocal protein from cell extracts in in vitro pull-down experiments (data not shown). Therefore, despite the interaction between a partial cDNA of Ajuba and a domain of the EPO-R cytoplasmic tail in yeast, the two full-length proteins did not interact in vitro or in vivo. Nonetheless, many features of the Ajuba protein sequence (e.g., LIM domains and amino-terminal SH3 recognition motifs) and developmental pattern of expression prompted us to determine the cellular functions for Ajuba.

Ajuba is a cytosolic protein, not found at sites of focal adhesion or associated with the actin cytoskeleton. To determine the subcellular distribution of Ajuba, immunofluorescence analysis was performed. NIH 3T3 fibroblast cell lines expressing Myc-tagged full-length Ajuba (3T3.Ajuba), Myc-tagged pre-LIM domain of Ajuba (the N terminus) (3T3.PreLIM), or Myc-tagged LIM domains of Ajuba (all three LIM domains in the C terminus) (3T3.LIM) were generated. NIH 3T3 cells do not express Ajuba mRNA or protein (data not shown). Results of immunofluorescence studies with anti-Myc antiserum and Ajuba-containing 3T3 cell lines are presented in Fig. 4. No Myc expression was detected in cells transfected with an empty vector (Fig. 4A). In cells containing full-length Myc-Ajuba, the protein was found predominantly in the cytosol (Fig. 4B). There was no nuclear staining; however, trace staining of the cell surface was evident. Subcellular fractionation studies using F9 cells, which express endogenous Ajuba, gave identical results (data not shown). 3T3 cells con-

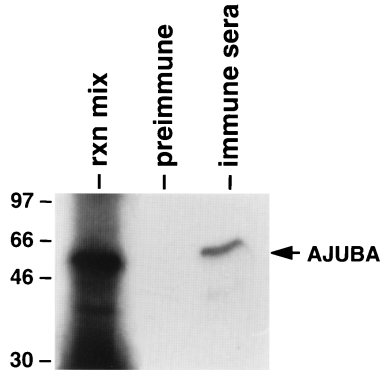

FIG. 3. Ajuba cDNA encodes a protein of 55 kDa specifically recognized by anti-Ajuba immune serum. The cDNA of Ajuba, clone 3B, was subcloned into pBS K/S$^-$; 1 mg of linearized plasmid was transcribed and translated in the presence of [^{35}S]methionine. In lane 1, 1/15 of final reaction (rxn) volume was loaded; in lane 2, 1/4 of the translation reaction was diluted to 1 ml in lysis buffer and 5 μl of preimmune serum was added, followed by protein A-agarose; in lane 3, 1/4 of translation product was diluted to 1 ml in lysis buffer and 5 μl of affinity purified anti-Ajuba immune serum was added, followed by protein A-agarose. Samples were run on an SDS–8% polyacrylamide gel under reducing conditions, the gel was dried, and autoradiography was performed. The arrowhead on the right indicates the mobility of Ajuba protein product. Mobility of molecular weight standards is indicated in kilodaltons on the left.

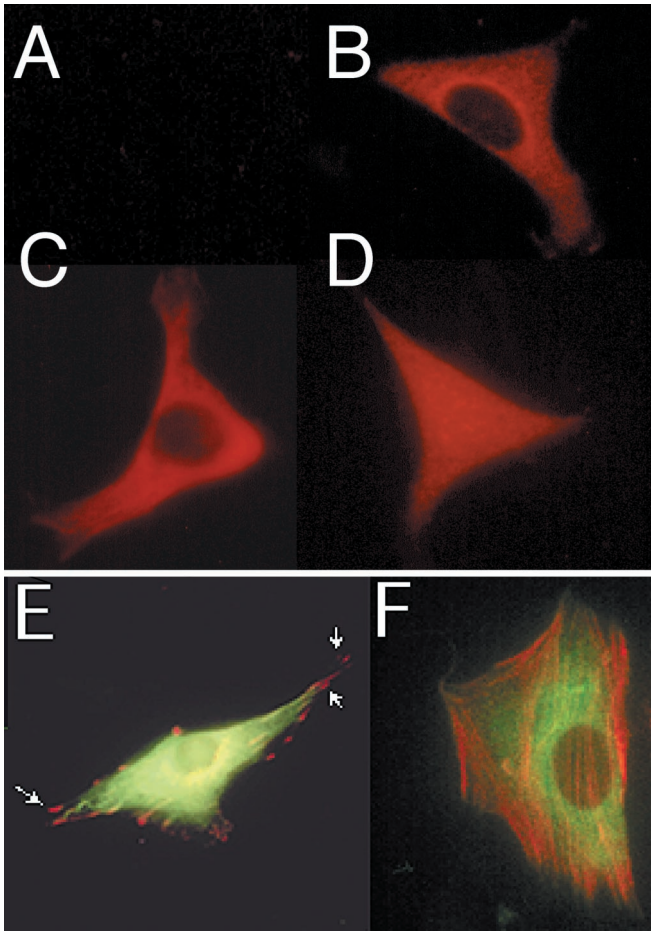

FIG. 4. Immunofluorescence analysis of NIH 3T3 fibroblasts expressing Ajuba isoforms. Immunofluorescence was performed as described in Materials and Methods. (A to D) Single immunofluorescence with anti-Myc antiserum; (E) dual immunofluorescence with anti-Myc (green) and antipaxillin (red) antisera; (F) dual immunofluorescence with anti-Myc antiserum (green) and rhodamine-conjugated phalloidin (red). Cells in panel A have been transfected with control empty expression vectors; cells in panel B contain Myc-tagged wild-type Ajuba; cells in panel C contain Myc-tagged pre-LIM Ajuba; cells in panel D contain Myc-tagged LIM Ajuba; cells in panels E stably express Myc-tagged wild-type Ajuba and were transiently transfected with a paxillin-containing plasmid prior to immunofluorescence; cells in panel F contain Myc-tagged Ajuba. Arrows in panel E identify sites of focal adhesions to the slides. Panel E has been slightly overexposed to visualize endogenous paxillin. In all other panels, exposure times are equivalent.

taining Myc–pre-LIM Ajuba expressed the protein only in the cytosol, in a pattern similar to cells containing full-length Ajuba (Fig. 4C). In cells containing only the three LIM domains found at the C terminus of Ajuba, significant amounts of protein were detected in the nucleus as well as throughout the cytosol (Fig. 4D).

Since two closely related group 3 LIM proteins, zyxin and paxillin, are found at sites of adhesion between cells and the substratum, we performed dual immunofluorescence on Myc-Ajuba-containing 3T3 cells transiently transfected with paxillin (Fig. 4E). No colocalization of Ajuba and paxillin was observed at sites of focal adhesion. Zyxin has been shown to also associate with the actin cytoskeleton (9). To determine if Ajuba colocalized with actin filaments in the cytosol, 3T3 cells containing Myc-Ajuba were costained with anti-Myc antiserum and phalloidin to detect actin filaments (Fig. 4F). We did not observe any colocalization of Ajuba with the actin filaments.

This analysis demonstrated that like other group 3 LIM proteins, Ajuba was predominantly a cytosolic protein, and a small amount may be associated with the cell surface membrane. However, in contrast to other group 3 LIM proteins, Ajuba did not localize to sites of cellular adhesion to substratum, nor did it associate with actin filaments. Interestingly, removal of the amino terminus, including a putative NES, resulted in the accumulation of the LIM domains in the nucleus.

Ajuba associates with Grb2 in vitro and in vivo. The amino-terminal half of Ajuba contained two proline-rich regions that correspond to potential SH3 recognition motifs (Fig. 1) (1, 15). To determine if cytosolic SH3-containing proteins might associate with Ajuba, we added various SH3-containing GST fusion proteins to ES cell extracts. Following incubation, the GST fusion proteins were isolated with glutathione-agarose, the products were separated by SDS-PAGE and transferred to nitrocellulose, and immunoblotting with anti-Ajuba antiserum was performed. This in vitro analysis demonstrated that Grb2 (Fig. 5A, lane 3) and related Grap (14) (Fig. 6) associated with Ajuba, whereas GST alone, GST-Nck, GST-Lck, and GST-Vav did not (Fig. 5A, lanes 2 and 4 to 6).

To determine if Ajuba and Grb2 associated in vivo, 3T3 cells containing Myc-Ajuba were deprived of serum overnight and then stimulated with serum for 15 min. Detergent-soluble cell extracts were prepared and immunoprecipitated with anti-Grb2 antiserum followed by immunoblotting of products with anti-Myc antiserum. This in vivo analysis indicated that cellular Ajuba associated with Grb2 following serum stimulation (Fig. 5B, lane 4), whereas under these conditions no association was detected in cells starved of serum (Fig. 5B, lane 3). This analysis was also carried out in ES and F9 cells, which contain endogenous Ajuba. As observed with 3T3.Ajuba cells, expressing exogenous Ajuba, there was an association between Ajuba and Grb2 (data not shown). Thus, Ajuba associated with Grb2 in vitro, and more importantly, in vivo.

The association between Ajuba and Grb2 was mediated by the N-terminal pre-LIM domain of Ajuba and either SH3 domain of Grb2. To more precisely define the regions of Ajuba required for the interaction with Grb2, we performed in vitro pull-down experiments. Purified GST-Grb2 and GST-Grap fusion proteins were added to extracts from Myc–pre-LIM Ajuba-containing 3T3 cells or Myc-LIM Ajuba-containing 3T3 cells. As negative controls, GST alone and GST-Vav fusion proteins were added to the same cell extracts. Results of these experiments are presented in Fig. 6A. GST-Grb2 and GST-Grap interacted with the pre-LIM domain of Ajuba (lanes 3 and 4). There was no interaction between GST-Grb2 or GST-Grap and the LIM domains of Ajuba (lanes 8 and 9). GST alone (lanes 2 and 7) or GST-Vav fusion protein (lanes 5 and 10) did not interact with either domain of Ajuba. Next, GST-Ajuba, GST–pre-LIM Ajuba, and GST-LIM Ajuba fusion proteins were added to F9 cell extracts and following incubation were isolated by incubation with glutathione-agarose beads. Bound products were separated by SDS-PAGE, transferred to nitrocellulose, and immunoblotted with anti-Grb2 antiserum. Results of these experiments are presented in Fig. 6B. GST-Ajuba and GST–pre-LIM Ajuba bound Grb2 (lanes 3 and 4), whereas GST alone and GST-LIM domains of Ajuba did not (lanes 2 and 5). These analyses demonstrated that it was the pre-LIM domain of Ajuba, not the LIM domains, that mediate the interaction with Grb2.

We next determined which domains of Grb2 or Grap interact with Ajuba. GST fusion proteins containing full-length Grb2, Grb2 with inactivating mutations in the C-terminal, N-terminal, or both SH3 domains (36), full-length Grap, the

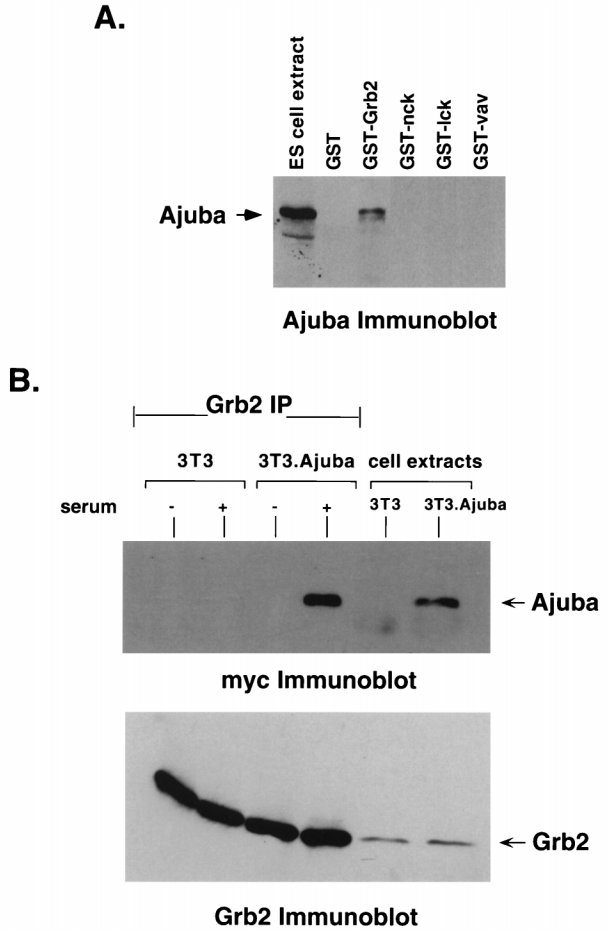

FIG. 5. Ajuba associates with Grb2 in vitro and in vivo in a serum-dependent manner. (A) ES cell extracts (ca. 10 million cells per lane) were incubated with approximately 5 μg of the indicated fusion proteins. Bound products were isolated with glutathione-agarose beads and resolved on an SDS–8% polyacrylamide gel under reducing conditions, transferred to nitrocellulose, and immunoblotted with anti-Ajuba antiserum. The arrow on the left identifies the mobility of endogenous Ajuba in ES cell extracts (lane 1). (B) 3T3 fibroblasts (lanes 1 and 2) or 3T3 fibroblasts containing Myc-Ajuba (lanes 3 and 4) were incubated overnight in serum-free medium and then either lysed (−, lanes 1 and 3) or incubated with medium containing 50% serum for 15 min at 37°C and then lysed (+, lanes 2 and 4). Extracts from approximately 20 million cells were immunoprecipitated with anti-Grb2 antiserum (lanes 1 to 4), resolved by SDS-PAGE, transferred to nitrocellulose, and immunoblotted with anti-Myc antiserum (upper panel). Lanes 5 and 6 are cell extracts from approximately 0.5 million 3T3 and 3T3.myc-Ajuba cells, respectively. Subsequently the blot was stripped and reprobed with anti-Grb2 antiserum. Proteins were visualized by enhanced chemiluminescence. Arrows on the right indicate the expected mobilities of Myc-Ajuba and Grb2.

N-terminal SH3 domain of Grap, or the C-terminal SH3 domain of Grap (14) were added to cell extracts from 3T3 cells containing Myc-tagged pre-LIM Ajuba. Anti-Myc immunoblotting of bound products was performed. Results of this experiment are presented in Fig. 6C. For an interaction between Grb2 or Grap and pre-LIM Ajuba to occur, a functional SH3 domain, either N terminal (lanes 5 and 8) or C terminal (lanes 4 and 9) or both (lanes 3 and 7), was required. When both SH3 domains of Grb2 were nonfunctional, pre-LIM Ajuba did not bind (lane 6). This result demonstrated that either SH3 domain of Grb2 could mediate the interaction between Grb2 and Ajuba.

Ajuba expression enhances MAP kinase activity. Grb2 is an adapter protein that couples signals from activated cell surface growth factor receptors or other activated cytosolic signaling intermediates to the activation of Ras and subsequently to MAP kinase activation (24). To determine if the interaction between Ajuba and Grb2 is functionally significant, we tested whether expression of Ajuba could affect MAP kinase activity.

Fibroblast 3T3 cell clones expressing Ajuba, the pre-LIM domain of Ajuba, or the three LIM domains of Ajuba, and control 3T3.Neo cells (derived from transfection with an empty vector), were deprived of serum and then stimulated with 10% serum for 15 min. Cells were then lysed, and MAP kinase activity present in equal amounts of protein from each sample was determined by immunoprecipitation of ERK and by in vitro kinase reactions performed with the bound material and MBP as a substrate. In control cells, minimal MAP kinase was present following serum starvation (Fig. 7A, lane 1). After stimulation with 10% serum, MAP kinase activity was increased (lane 4), as expected. In cells containing Ajuba, serum starvation overnight did not completely suppress MAP kinase activity (lane 3). MAP kinase activity was 10-fold greater than in control cells, a level of MAP kinase activity observed in control cells stimulated with serum. Addition of 10% serum to these cells stimulated further MAP kinase activity (lane 6) to a level fivefold higher than that in control cells following serum stimulation. This pattern of MAP kinase activity mapped to the pre-LIM domain of Ajuba since cells containing pre-LIM Ajuba (Fig. 7A, lanes 2 and 5) gave a response similar to that of cells expressing full-length Ajuba, whereas cells expressing only the LIM domains of Ajuba (Fig. 7B, lanes 2 and 4) exhibited MAP kinase activity profiles similar to those of control mock-transfected 3T3 cells (Fig. 7B, lanes 1 and 3). This result correlates precisely to the domain of Ajuba required to mediate the interaction between Ajuba and Grb2. Thus, in cells expressing exogenous Ajuba or the pre-LIM domain, but not the LIM domains, of Ajuba, MAP kinase activity persisted despite serum starvation, and the response to serum was exaggerated.

Ajuba expression in *Xenopus* oocytes promotes meiotic maturation in a Grb2- and Ras-dependent manner. To demonstrate that the enhanced MAP kinase activity observed in fibroblasts expressing Ajuba was functionally relevant in a physiological context, we tested whether expression of Ajuba in fully developed *Xenopus* oocytes could affect their meiotic maturation. In response to progesterone and insulin, fully grown *Xenopus* oocytes (which are arrested at the first meiotic prophase of the cell cycle) resume the meiotic process leading to the production of the unfertilized egg. MAP kinase activation is an essential component of this response pathway (22). Fully grown stage VI oocytes were isolated from *Xenopus* ovaries and microinjected with in vitro-transcribed Myc-Ajuba, Myc–pre-LIM Ajuba, or Myc-LIM Ajuba mRNA or, as a negative control, mRNA produced by in vitro transcription of the parental pCS2 vector. Following recovery, oocytes were treated with progesterone or insulin and at various time points scored for the presence of GVBD, as an indicator of meiotic progression. In the absence of inducer, some batches of oocytes injected with Ajuba underwent spontaneous maturation (data not shown). However, reproducibly, the presence of Ajuba in oocytes was found to increase the number that underwent GVBD in response to progesterone (Fig. 8A) or insulin (Fig. 8B). Fifty-five percent of oocytes injected with control mRNA underwent GVBD, whereas 80% of oocytes injected with Myc-Ajuba mRNA underwent GVBD (Fig. 8A). This augmented response mapped to the pre-LIM domain of Ajuba, not the LIM domains, since 65% of oocytes injected

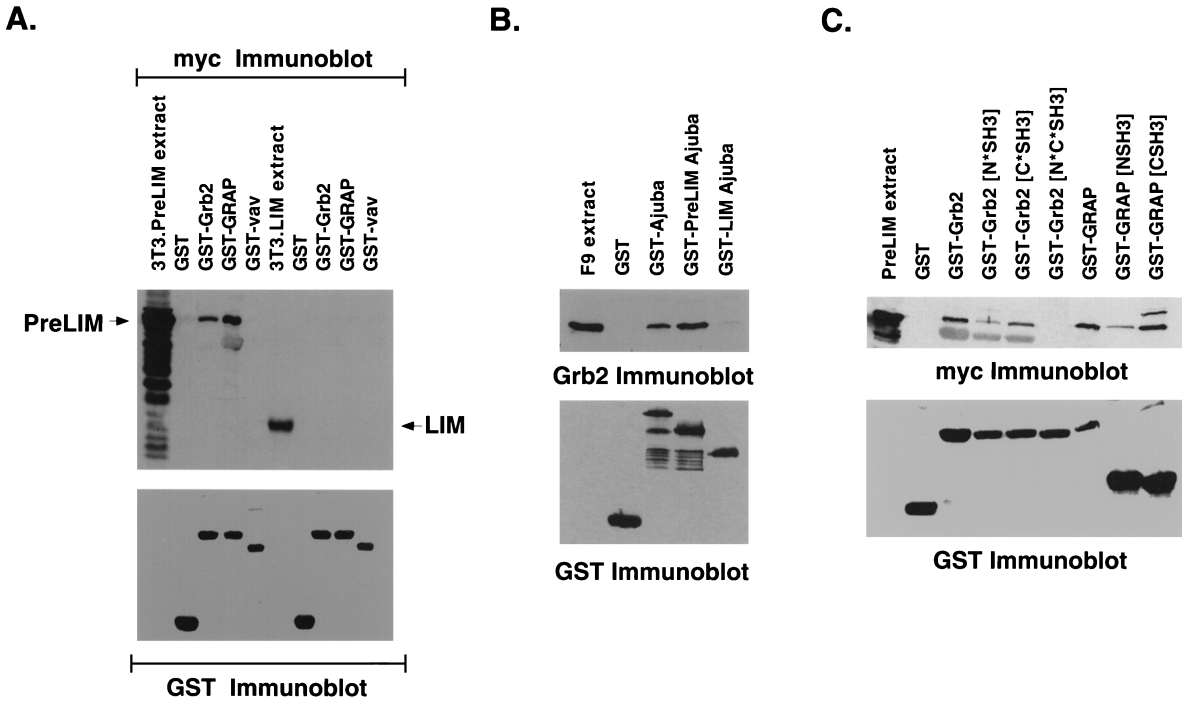

FIG. 6. The pre-LIM domain of Ajuba and the SH3 domains of Grb2 mediate the association of Ajuba and Grb2. (A) Extracts from approximately 10 million 3T3.PreLIM Ajuba cells (lanes 2 to 5) or 3T3.LIM Ajuba cells (lanes 7 to 10) were incubated with approximately 5 μg of the indicated fusion proteins. Bound products were isolated with glutathione-agarose beads and resolved on an SDS–8% polyacrylamide gel under reducing conditions, transferred to nitrocellulose, and immunoblotted with anti-Myc antiserum (upper panel). Subsequently the blot was stripped and reprobed with anti-GST antiserum to indicate the level of fusion proteins present in each sample (lower panel). Lane 1 is a detergent-soluble extract from ca. 0.5 million 3T3 cells containing the Myc-tagged pre-LIM domain of Ajuba. The arrow on the left identifies the expected mobility of the Myc-pre-LIM protein. Lane 6 is an extract from 3T3 cells containing Myc-tagged LIM domains of Ajuba. The arrow on the right identifies the expected mobility of the Myc-LIM only protein. (B) Extracts from approximately 10 million F9 cells were incubated with approximately 5 μg of the indicated fusion proteins (lanes 2 to 5). Bound products were isolated with glutathione-agarose beads and resolved on an SDS–8% polyacrylamide gel under reducing conditions, transferred to nitrocellulose, and immunoblotted with anti-Grb2 antiserum (upper panel). Subsequently the blot was stripped and reprobed with anti-GST antiserum to indicate the level of fusion protein present in each sample (lower panel). Lane 1 is a detergent-soluble extract from ca. 0.5 million F9 cells. (C) Extracts from approximately 10 million 3T3.Pre-LIM Ajuba cells were incubated with approximately 5 μg of the indicated fusion proteins (lanes 2 to 9). Bound products were isolated with glutathione-agarose beads and resolved on an SDS–8% polyacrylamide gel under reducing conditions, transferred to nitrocellulose, and immunoblotted with anti-Myc antiserum (upper panel). Subsequently the blot was stripped and reprobed with anti-GST antiserum to indicate the level of fusion protein present in each sample (lower panel). Lane 1 is a detergent-soluble extract from ca. 0.5 million 3T3 cells containing Myc–pre-LIM Ajuba.

with Myc–pre-LIM Ajuba underwent GVBD whereas only 30% of oocytes injected with Myc-LIM Ajuba underwent GVBD (Fig. 8A).

To determine if Grb2 contributed to this result, oocytes were coinjected with Ajuba and Grb2 mRNA or with Ajuba and an inactivated isoform of Grb2 in which both SH3 domains are nonfunctional (Grb2 SH3-N,C). Following coinjection of Ajuba and Grb2, ca. 90% of oocytes underwent GVBD in response to progesterone (a value significantly greater than for oocytes injected with Ajuba alone), whereas coinjection of Ajuba and Grb2 SH3-N,C resulted in only 60% GVBD (a value comparable to that for control oocytes) (Fig. 8A). Looked at another way, Grb2 SH3-N,C inhibited the ability of Ajuba to promote GVBD in response to progesterone, whereas wild-type Grb2 further enhanced GVBD in oocytes injected with Ajuba mRNA. Grb2 coinjection with pre-LIM Ajuba also appeared to enhance GVBD; however, this difference was not significantly different from that for oocytes injected with pre-LIM alone.

Thus, Ajuba significantly enhanced meiotic progression of oocytes in response to progesterone. This response mapped to the pre-LIM domain of Ajuba and was further augmented when Grb2, but not an inactivated isoform of Grb2, was coinjected with Ajuba, indicating that the ability of Ajuba to promote GVBD was Grb2 dependent.

Since a major pathway by which Grb2 couples signals to the activation of MAP kinase is dependent on the activation of Ras, we tested whether a dominant inhibitory form of Ras (RasN17) would block the enhanced GVBD observed in oocytes injected with Ajuba (Fig. 8B). Insulin-induced GVBD occurs in a Ras-dependent manner, whereas progesterone-induced GVBD is Ras independent (35) (Fig. 8B). In the presence of Ajuba, 25% more oocytes than controls underwent GVBD in response to insulin or progesterone. When RasN17 mRNA was coinjected with Ajuba mRNA, this 25% gain in GVBD was completely blocked (Fig. 8B). The number of progesterone-treated oocytes undergoing GVBD was similar to the number of control oocytes. Likewise, there was no difference between control/RasN17 and Ajuba/RasN17-injected insulin-treated oocytes. This analysis indicates that the ability of Ajuba to promote GVBD was mediated in a Ras-dependent manner.

To examine the kinetics of progesterone-mediated meiotic maturation of oocytes injected with Ajuba compared to controls, and to correlate this to expression of Ajuba protein and MAP kinase activation, we performed a detailed time course of GVBD development with concurrent biochemical analysis for Ajuba expression and MAP kinase activity. Compared with control oocytes, oocytes injected with Myc-Ajuba mRNA initiated GVBD and achieved maximal levels of GVBD at earlier

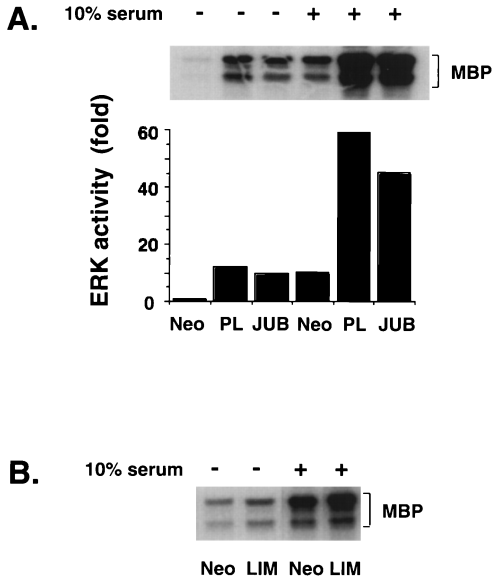

FIG. 7. Ajuba expression in 3T3 cells results in an augmentation of MAP kinase activity. Cells were incubated in serum-free medium overnight and then either lysed (−) or stimulated for 15 min at 37°C with medium containing 10% serum and then lysed (+). The protein concentration of each sample was determined, extracts containing equal amounts of protein were immunoprecipitated with antiserum against ERK, and in vitro kinase reactions were performed with MBP as the substrate. Products were resolved by SDS-PAGE under reducing conditions, the gel was dried, and autoradiography was performed. Gels were scanned, and the relative quantities of phosphorylated MBP were determined. (A) Lanes 1 and 4, control 3T3.Neo cells; lanes 2 and 5, 3T3.PreLIM Ajuba cells; lanes 3 and 6, 3T3.Ajuba cells. (B) Lanes 1 and 3, control 3T3.Neo cells; lanes 2 and 4, 3T3.LIM cells.

times (Fig. 9A). Ajuba-injected oocytes expressed Myc-Ajuba protein as early as 4 h following progesterone addition, with maximal levels at 8 h, as determined by Myc immunoblotting of extracts from individual oocytes (Fig. 9D). MAP kinase activation paralleled the expression of Ajuba, as determined by immunoblotting individual oocyte extracts with an antibody that recognizes activated MAP kinase (New England Biolabs) (Fig. 9B). In addition, the peak of MAP kinase activity in Ajuba-injected oocytes preceded that observed in control oocytes (Fig. 9C). Expression of Ajuba protein did not affect the level of ERK protein expression (Fig. 9E). Expression of Ajuba protein and activation of MAP kinase activity directly correlated with the earlier onset of GVBD observed in oocytes injected with Ajuba mRNA (Fig. 9A).

DISCUSSION

We have identified and characterized a new cytosolic LIM protein, Ajuba. Ajuba specifically associated with Grb2 in vitro and in vivo. The interaction between these proteins was mediated by either SH3 domain of Grb2 and the N-terminal proline-rich pre-LIM domain of Ajuba. In fibroblasts expressing Ajuba, MAP kinase activity persisted despite serum starvation and upon serum stimulation generated levels fivefold higher than that seen in control cells. Finally, when Ajuba was expressed in fully developed *Xenopus* oocytes, it promoted meiotic maturation in a Grb2- and Ras-dependent manner.

Previous work has demonstrated that cytosolic group 3 LIM proteins may participate in growth factor signaling pathways. Enigma interacts with the cytoplasmic tail of the Ret/ptc2 receptor tyrosine kinase (12). This interaction is mediated by the second LIM domain of Enigma and is required for the mitogenic activity of Ret. Which Ret-induced intracellular signaling pathways are affected by this interaction has not been explored, however. The third LIM domain of Enigma also interacts with a tyrosine-based internalization motif in the cytoplasmic tail of the insulin receptor (44, 45). While this interaction may be important in regulating receptor endocytosis or intracellular receptor trafficking between organelles, it most likely does not affect the signaling properties of the insulin receptor, although this has not been formally proven. Proteins interacting with the N-terminal, pre-LIM domain of Enigma have not been identified, and the cellular function of this domain of Enigma has not been well studied.

The LIM domains of paxillin mediate its interaction with the cytoskeleton (37). Paxillin is heavily tyrosine phosphorylated in response to integrin-mediated cell adhesion, peptide growth factors, and the $p210^{bcr/abl}$ protein (8, 32, 46). The pre-LIM, proline-rich, N-terminal domain of paxillin has been shown to bind to the SH3 domain of $p60^{c\text{-}src}$ and the SH2 domain of v-Crk in vitro (43) (6), but the functional significance of these interactions has not been established.

Zyxin is a low-abundance phosphoprotein that colocalizes with integrin receptors at sites of focal adhesion (5). The SH3 domain of Vav has been shown to interact with the proline-rich pre-LIM region of zyxin in vitro; however, it has not been determined whether this interaction occurs in vivo or whether there is any functional consequence of this interaction (18). Thus, the ability of zyxin to modulate growth factor signaling remains unclear.

Here we have shown that a new group 3 LIM protein, Ajuba, affects specific intracellular signaling pathways in response to extracellular stimuli. Ajuba interacted with Grb2 in fibroblasts, and fibroblasts expressing Ajuba exhibited augmented MAP kinase activity following both serum starvation and serum stimulation. When expressed in *Xenopus* oocytes, Ajuba promoted meiotic maturation, a process dependent on the activation of MAP kinase. The ability of Ajuba to promote meiotic maturation was dependent on Grb2. First, oocytes injected with both Ajuba and Grb2 mRNA exhibited more GVBD than oocytes injected with Ajuba alone. Second, oocytes injected with both Ajuba and an inactive form of Grb2 did not exhibit enhanced meiotic maturation. Finally, injection of oocytes with dominant negative Ras blocked the ability of Ajuba to promote GVBD. A major pathway by which Grb2 leads to the activation of MAP kinase is through the activation of Ras (13, 24), which suggests that Ajuba-mediated meiotic progression was Grb2 and Ras dependent. Importantly, the ability of Ajuba to promote meiotic maturation in oocytes temporally coincided with the level of Ajuba protein expression. In the presence of Ajuba, MAP kinase was activated at earlier time points and to a greater magnitude, thereby resulting in the onset of GVBD at earlier times and an increase in the total number of oocytes that underwent GVBD.

The effect of Ajuba expression on meiotic progression in mature oocytes is similar to that observed for the recently described kinase Eg2 (2). Overexpression of Eg2 mRNA in fully grown oocytes shortens the time between progesterone stimulation and the entry into the meiosis. In the presence of Eg2, the time to appearance of Mos protein is shortened. The premature elevation of Mos leads to early activation of MAP kinase and hence meiotic progression. Progesterone-mediated meiotic progression occurs in a Ras-independent manner (35). In contrast to Eg2, Ajuba does not induce premature elevations in Mos protein (data not shown), yet it does lead to premature activation of MAP kinase in a Ras-dependent manner.

The association between Ajuba and Grb2 in fibroblasts was found to occur in a serum-dependent manner, yet fibroblasts

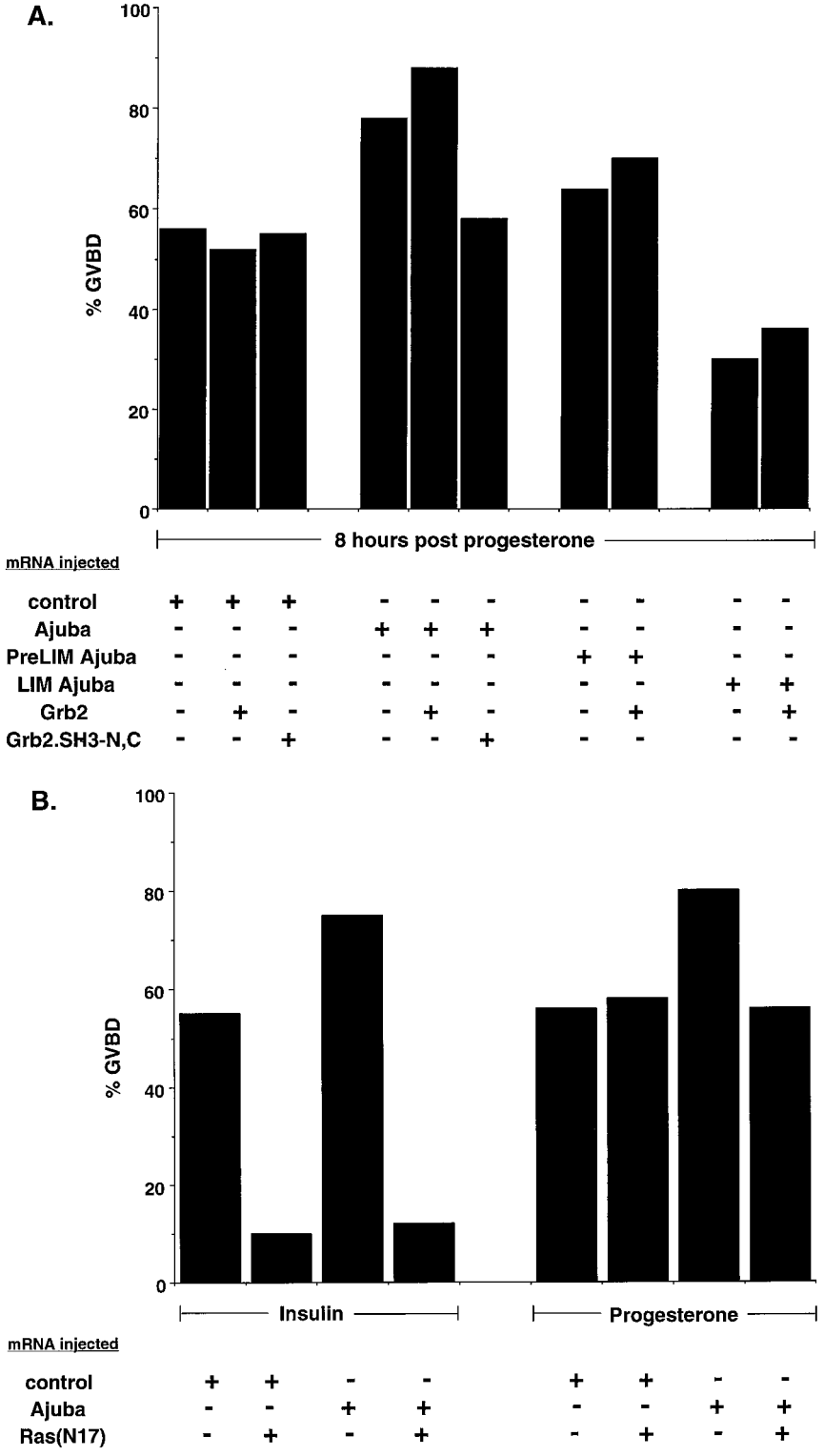

FIG. 8. Ajuba expression in *Xenopus* oocytes promotes meiotic maturation in a Grb2- and Ras-dependent manner. (A) Mature *Xenopus* oocytes were injected with 50 ng of in vitro-transcribed mRNA as described in Materials and Methods. After recovery, healthy oocytes were cultured in medium containing 3 μM progesterone; the percentage of oocytes undergoing GVBD was scored after 8 h. In all samples, between 40 and 50 oocytes were scored. For each set, multiple experiments were performed and a representative set is shown. The mRNAs injected for each column are listed below the graph. (B) The first group (columns 1 to 4) of oocytes were treated with insulin, and the percentage undergoing GVBD was scored at 20 h posttreatment. The second group (columns 5 to 8) were treated with progesterone, and the percentage undergoing GVBD was scored 8 h after treatment. In all samples, between 40 and 50 oocytes were scored. For each set, multiple experiments were performed and a representative set is shown. The mRNAs injected for each column are listed below the graph.

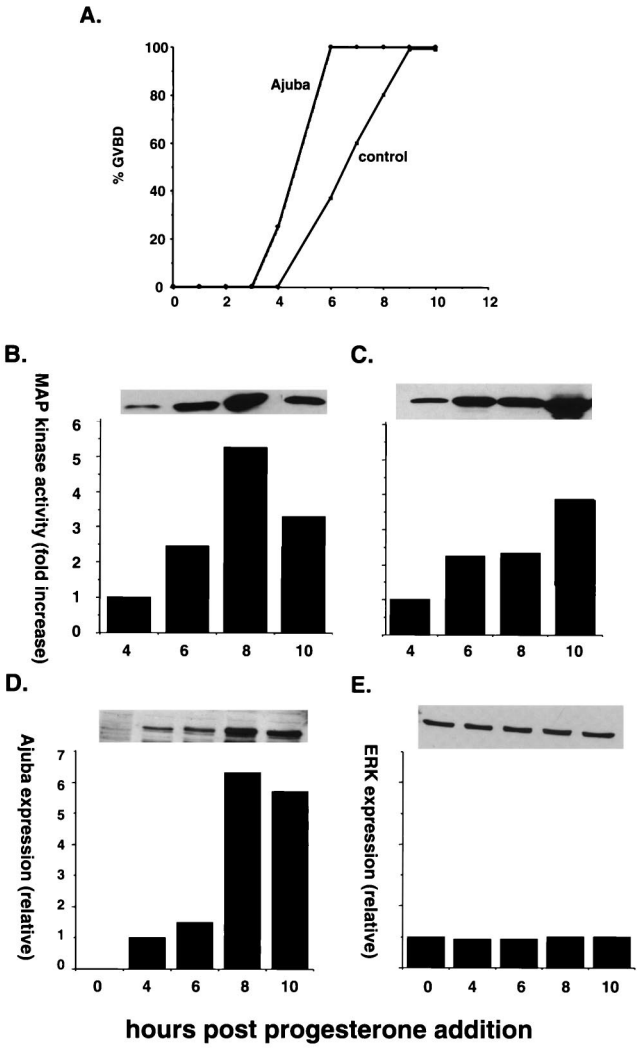

FIG. 9. Ajuba expression in oocytes results in earlier onset of meiotic maturation (GVBD) coinciding with earlier activation of MAP kinase activity. Batches of oocytes were injected with water (control) or Ajuba mRNA. After recovery, healthy oocytes were cultured in medium containing 3 μM progesterone. Oocytes were scored hourly for the presence of GVBD until a maximal level was reached (A). The percentage of oocytes that had undergone GVBD at 10 h was set as 100%. Results at each time point are presented as a percentage of the maximal level. At selected time points, oocytes were picked and lysed. (B and C) MAP kinase activity determined by immunoblotting with an antiserum that recognizes activated MAP kinase. (B) Ajuba-injected oocytes; (C) control injected oocytes. The relative amount of Ajuba protein expression was determined by immunoblotting with anti-Myc antiserum (D). ERK protein level was determined by immunoblotting with anti-ERK antiserum (E). Panels D and E show results from Ajuba-injected oocytes.

containing Ajuba had elevated levels of MAP kinase activity following serum deprivation. This finding suggests that the enhanced MAP kinase activity in these cells is not entirely due to the association between Ajuba and Grb2. The interaction between Ajuba and Grb2 was found to be mediated by the either SH3 domain of Grb2 and the pre-LIM domain of Ajuba, which contain proline-rich SH3 recognition motifs. Typically SH3 interactions are independent of serum stimulation and raise the distinct possibility that some other, as yet unidentified protein(s) is present in the Grb2-Ajuba complex. These other proteins may contribute to MAP kinase activation independent of the association with Grb2 and explain the persistent MAP kinase activity observed in Ajuba-expressing fibroblasts starved of serum, whereas the excessive MAP kinase activity observed following serum stimulation may be due to the association between Ajuba and Grb2. It is tempting to speculate that this putative associated protein(s) may be recruited to the complex through an interaction with the LIM domains of Ajuba. Current work is directed at identifying cellular proteins that interact with the LIM domains of Ajuba.

Recently, Nix and Beckerle demonstrated that zyxin contains a functional NES and suggested that the NES is required to exclude zyxin from the nucleus (26). They also demonstrated that endogenous zyxin actually shuttles between the cytoplasm and nucleus. Ajuba also contains a strong putative NES, in a region of the protein complementary to the site of the NES present in zyxin (7, 21). Interestingly, when we removed the pre-LIM domain of Ajuba, including a putative NES, and expressed this LIM-only isoform of Ajuba in fibroblast cells, we observed that a significant proportion of the LIM-only Ajuba was now present in the nucleus. Similarly, transient overexpression of LIM-only Ajuba in HeLa cells resulted in the presence of the protein in the nuclear fraction, whereas full-length Ajuba or pre-LIM Ajuba proteins remained in the detergent-soluble cytosol/membrane fraction (data not shown). Therefore, like zyxin, Ajuba may shuttle between the nucleus and cytoplasm and thus serve to communicate signals between these two cellular compartments.

ACKNOWLEDGMENTS

We thank Jim Palis, David B. Wilson, and Markku Heikinheimo for evaluation of in situ results and helpful discussions; Andrey Shaw, Andy Chan, and Gensheng Feng for readily providing reagents; and Andrey Shaw for helpful comments and criticisms.

This work was supported in part by the Robert Steel Foundation for Pediatric Cancer Research (R.K.G.), by NIH grant RO1 CA75315 (G.D.L.), and by a grant from Abbott Laboratories (G.D.L.). G.D.L. was a scholar of the James S. McDonnell Foundation.

REFERENCES

1. **Alexandropoulos, K., G. Cheng, and D. Baltimore.** 1995. Proline-rich sequences that bind to src homology 3 domains with individual specificities. Proc. Natl. Acad. Sci. USA **92:**3110–3114.
2. **Andresson, T., and J. V. Ruderman.** 1998. The kinase Eg2 is a component of the xenopus oocyte progesterone-activated signaling pathway. EMBO J. **17:**5627–5637.
3. **Arber, S., G. Halder, and P. Caroni.** 1994. Muscle LIM protein, a novel essential regulator of myogenesis, promotes myogenic differentiation. Cell **79:**221–231.
4. **Beckerle, M. C.** 1988. Identification of a new protein localized at sites of cell-substratum adhesion. J. Cell Biol. **103:**1679–1687.
5. **Beckerle, M. C.** 1997. Zyxin: zinc fingers at sites of cell adhesion. BioEssays **19:**949–957.
6. **Birge, R. B., E. Fajardo, C. Reichman, S. Shoelson, Z. Songyang, L. C. Cantley, and H. Hanafusa.** 1993. Identification and characterization of a high-affinity interaction between v-Crk and tyrosine-phosphorylated paxillin in CT10-transformed fibroblasts. Mol. Cell. Biol. **13:**4648–4656.
7. **Bogerd, H. P., R. A. Fridell, R. E. Benson, J. Hua, and B. R. Cullen.** 1996. Protein sequence requirements for function of the human T-cell leukemia virus type I Rex nuclear export signal delineated by a novel in vivo randomization-selection assay. Mol. Cell. Biol. **16:**4207–4214.
8. **Burridge, K., K. Fath, T. Kelly, G. Nuckolls, and C. Turner.** 1988. Focal adhesions: transmembrane junctions between the extracellular matrix and the cytoskeleton. Annu. Rev. Cell Biol. **4:**487–525.
9. **Crawford, A. W., J. D. Pino, and M. C. Beckerle.** 1994. Biochemical and molecular characterization of the chicken cysteine-rich protein, a developmentally regulated LIM-domain protein that is associated with the actin cytoskeleton. J. Cell Biol. **124:**117–127.
10. **Dawid, I. B., J. J. Breen, and R. Toyama.** 1998. LIM domains: multiple roles as adapters and functional modifiers in protein interactions. Trends Genet. **14:**156–162.
11. **Doetschman, T., H. Eistetter, M. Katz, W. Schmidt, and R. Kemler.** 1985. The in vitro development of blastocyst derived embryonic stem cell lines: formation of visceral yolk sac, blood islands, and myocardium. J. Embryol. Exp. Morphol. **87:**27.

12. **Durick, K., R.-Y. Wu, G. N. Gill, and S. S. Taylor.** 1996. Mitogenic signaling by Ret/ptc2 requires association with Enigma via a LIM domain. J. Biol. Chem. **271:**12691–12694.
13. **Egan, S. E., B. W. Giddings, M. W. Brooks, L. Buday, A. M. Sizeland, and R. A. Weinberg.** 1993. Association of Sos Ras exchange protein with Grb2 is implicated in tyrosine kinase signal transduction and transformation. Nature **363:**45–51.
14. **Feng, G.-S., Y.-B. Ouyang, D.-P. Hu, Z.-Q. Shi, R. Gentz, and J. Ni.** 1996. Grap is a novel SH3-SH2-SH3 adapter protein that couples tyrosine kinases to the Ras pathway. J. Biol. Chem. **271:**12129–12132.
15. **Feng, S., J. K. Chen, H. Yu, J. A. Simon, and S. L. Schreiber.** 1994. Two binding orientations for peptides to the src SH3 domain: development of a general model for SH3-ligand interactions. Science **266:**1241–1247.
16. **Freyd, G., S. K. Kim, and H. R. Horvitz.** 1990. Novel cysteine-rich motif and homeodomain in the product of the C. elegans. cell lineage gene lin-11. Nature **344:**867–879.
17. **Gill, G. N.** 1995. The enigma of LIM domains. Structure **3:**1285–1289.
18. **Hobert, O., J. W. Schilling, M. C. Beckerle, A. Ullrich, and B. Jallal.** 1996. SH3 domain-dependent interaction of the proto-oncogene product Vav with the focal contact protein Zyxin. Oncogene **12:**1577–1581.
19. **Hogan, B., R. Beddington, F. Constantini, and E. Lacy.** 1994. Manipulating the mouse embryo: a laboratory manual. Cold Spring Harbor Laboratory, Cold Spring Harbor, N.Y.
20. **Karlsson, O., S. Thor, T. Njorberg, H. Ohlsson, and T. Edlund.** 1990. Insulin gene enhancer binding protein Isl-1 is a member of a novel class of proteins containing both a homeo- and a Cys-His domain. Nature **344:**879–882.
21. **Kim, F. J., A. A. Beeche, J. J. Hunter, D. J. Chin, and T. J. Hope.** 1996. Characterization of the nuclear export signal of human T-cell lymphotropic virus type I Rex reveals that nuclear export is mediated by position variable hydrophobic interactions. Mol. Cell. Biol. **16:**5147–5155.
22. **Kosako, H., Y. Gotoh, and E. Nishida.** 1994. Regulation and function of the MAP kinase cascade in Xenopus oocytes. J. Cell Sci. **18:**115–119.
22a. **Kozak, M.** 1986. Point mutations define a sequence flanking the AUG initiator codon that modulates translation by eukaryotic ribosomes. Cell **44:**283–292.
23. **Lee, J., H. Choi, J. Gyuris, R. Brent, and D. Moore.** 1995. Two classes of proteins dependent on either the presence or absence of thyroid hormone for interaction with the thyroid hormone receptor. Mol. Endocrinol. **9:**243–254.
24. **Lowenstein, E. J., R. J. Daly, A. G. Batzer, W. Li, B. Margolis, R. Lammers, A. Ullrich, E. Y. Skolnik, D. Bar-Sagi, and J. Schlessinger.** 1992. The SH2 and SH3 domain-containing protein GRB2 links receptor tyrosine kinases to ras signaling. Cell **70:**431–442.
25. **Mizuno, K., I. Okano, K. Ohashi, K. Nunoue, K. Kuma, T. Miyata, and T. Nakamura.** 1994. Identification of a human cDNA encoding a novel protein kinase with two repeats of the LIM/double zinc finger motif. Oncogene **9:**1605–1612.
26. **Nix, D. A., and M. C. Beckerle.** 1997. Nuclear-cytoplasmic shuttling of the focal contact protein, zyxin: a potential mechanism for communication between sites of cell adhesion and the nucleus. J. Cell Biol. **138:**1139–1147.
27. **Oberlander, U., R. Adam, K. Berg, F. Seeber, and R. Lucius.** 1995. Molecular cloning and characterization of the filarial LIM domain proteins AvL3-1 and OvL3-1. Exp. Parasitol. **81:**592–599.
28. **Perez-Alvardo, G. C., C. Miles, J. W. Michelson, H. Louis, D. R. Winge, M. C. Beckerle, and M. F. Summers.** 1994. Structure of the carboxy-terminal LIM domain from the cysteine-rich protein CRP. Nat. Struct. Biol. **1:**388–398.
29. **Petit, M., R. Mols, E. Schoenmakers, N. Mandahl, and W. Van De Ven.** 1996. LPP, the preferred fusion partner gene of HMGIC in lipomas is a novel member of the LIM protein gene family. Genomics **36:**118–129.
30. **Reinhard, M., K. Jouvenal, D. Tripier, and U. Walter.** 1995. Identification, purification, and characterization of a zyxin-related protein that binds the focal adhesion and microfilament protein VASP. Proc. Natl. Acad. Sci. USA **92:**7956–7960.
31. **Sadler, I., A. W. Crawford, J. W. Michelsen, and M. C. Beckerle.** 1992. Zyxin and cCRP: two interactive LIM domain proteins associated with the cytoskeleton. J. Cell Biol. **119:**1573–1587.
32. **Salgia, R., J.-L. Li, S. H. Lo, B. Brunkhorst, G. S. Kansas, E. S. Sobhany, Y. Sun, E. Pisick, M. Hallek, T. Ernst, R. Tantravahi, L. B. Chen, and J. D. Griffin.** 1995. Molecular cloning of human paxillin, a focal adhesion protein phosphorylated by P210BCR/ABL. J. Biol. Chem. **270:**5039–5047.
33. **Sanchez-Garcia, I., and T. H. Rabbits.** 1993. LIM domain proteins in leukemia and development. Cancer Biol. **4:**349–358.
34. **Schmeichel, K. L., and M. C. Beckerle.** 1997. Molecular dissection of a LIM domain. Mol. Biol. Cell. **8:**219–230.
35. **Shibuya, E. K., J. Morris, U. R. Rapp, and J. V. Ruderman.** 1996. Activation of the Xenopus oocyte mitogen-activated protein kinase pathway by Mos is independent of Raf. Cell Growth Differ. **7:**235–241.
36. **Tanaka, M., R. Gupta, and B. J. Mayer.** 1995. Differential inhibition of signaling pathways by dominant-negative SH2/SH3 adapter proteins. Mol. Cell. Biol. **15:**6829–6837.
37. **Turner, C.** 1994. Paxillin: a cytoskeletal target for tyrosin kinases. BioEssays **16:**47–52.
38. **Turner, C., J. Glenney, and K. Burridge.** 1990. Paxillin: a new vinculin-binding protein present in focal adhesions. J. Cell Biol. **111:**1059–1068.
39. **Vojtek, A. B., S. M. Hollenberg, and J. A. Cooper.** 1993. Mammalian Ras interacts directly with the serine/threonine kinase Raf. Cell **74:**205–214.
40. **Warren, A. J., W. H. Colledge, M. Carlton, M. J. Evans, A. Smith, and T. H. Rabbitts.** 1994. The oncogenic cysteine-rich LIM domain protein Rbtn2 is essential for erythroid development. Cell **78:**45–57.
41. **Way, J. C., and M. Chalfie.** 1988. mec-3, a homeobox-containing gene that specifies differentiation of the touch receptor neurons in C. elegans. Cell **54:**5–16.
42. **Weng, D. E., R. A. Morgan, and J. D. Gearhart.** 1989. Estimates of mRNA abundance in the mouse blastocyst based on cDNA library analysis. Mol. Reprod. Dev. **1:**233–241.
43. **Weng, Z., J. A. Taylor, C. Turner, J. S. Brugge, and C. Seidel-Dugan.** 1993. Detection of Src homology 3-binding proteins, including paxillin, in normal and v-src-transformed Balb/c 3T3 cells. J. Biol. Chem. **268:**14956–14963.
44. **Wu, R.-Y., K. Durick, Z. Songyang, L. C. Cantley, S. S. Taylor, and G. N. Gill.** 1996. Specificity of LIM domain interactions with receptor tyrosine kinases. J. Biol. Chem. **271:**15934–15941.
45. **Wu, R. Y., and G. N. Gill.** 1994. The LIM domain recognition of a tyrosine-containing tight turn. J. Biol. Chem. **269:**25085–25090.
46. **Zachary, I., J. Sinnett-Smith, C. E. Turner, and E. Rozengurt.** 1993. Bombesin, vasopressin, and endothelin rapidly stimulate tyrosine phosphorylation of the focal adhesion-associated protein paxillin in Swiss 3T3 cells. J. Biol. Chem. **268:**22060–22065.